

Green synthesis of gold nanoparticles from *Prunus cerasifera pissardii nigra* leaf and their antimicrobial activities on some food pathogens

Abdulkerim Hatipoğlu

Department of Nutrition and Dietetics, Faculty of Health Sciences, Mardin Artuklu University, Mardin, Turkey

Abstract. In this study, a new and easy method for the biosynthesis of gold nanoparticles (AuNPs) with *Prunus cerasifera pissardii nigra* (PC) leaf extract as a reducing and stabilizing agent was presented. The nanoparticles were demonstrated a characteristic peak at the maximum wavelength of 535 nm with colour change as a result of the ultraviolet (UV)-visible spectrophotometer analysis data. Emission Scanning Electron Microscopy (FE-SEM), Transmission Electron Microscopy (TEM) and energy-dispersive X-ray spectroscopy (EDX) analyzes revealed that the crystal size of the synthesized AuNPs was below 20 nm and the morphological structure was mostly spherical. The size of the crystal structures of AuNPs was calculated as 17.94 nm from the X-ray diffraction (XRD) analysis data. Fourier Transform Infrared (FT-IR) Spectroscopy results confirmed the involvement of various biomolecules in the reduction and stabilization of PC-AuNPs. The zeta potential of the synthesized nanomaterial was measured as -27 mV. The average size of AuNPs was determined as 103.8 nm with Zetasizer. It was determined that AuNPs have strong inhibitory activity against *Escherichia coli*, *Staphylococcus aureus*, *Bacillus subtilis* and *Pseudomonas aeruginosa* and *Candida albicans*.

Key words: AuNPs, FE-SEM, TEM, EDX, XRD, MIC, Antimicrobial effect

Introduction

Scientific efforts to synthesize metal nanoparticles from natural sources have increased. For this purpose, many studies have been carried out on metal nanoparticles such as silver (1), platinum (2), iron (3), zinc oxide (4) and gold (5). Especially AuNPs attract great attention due to their oxidation resistance, easy synthesis and biocompatibility (6-9). AuNPs can be used in biomedicine (10), drug delivery, diagnostics, imaging (11), food packaging (12), and cosmetics (13).

AuNPs are generally reduced with stabilizing/reducing reagents such as hydrazine, sodium citrate, sodium borohydride, dimethyl formamide, folic acid and ascorbic acid, and then synthesized by surface modification with suitable capping ligands to prevent

spontaneous aggregation (14-16). However, many of the traditional methods use environmentally harmful chemicals and toxic capping agents. In addition, these methods are costly (17). To eliminate these negative situations, "green synthesis" studies in which metal nanoparticles are synthesized from plants (18), algae (19), fungi (20), bacteria (21) and viruses (22) have intensified in recent years.

In this study, a new and easy method for the biosynthesis of AuNPs with PC leaf extract as a reducing and stabilizing agent was introduced. To our knowledge, there is no documentation on the biosynthesis of AuNPs using PC. PC, also known as cherry plum, is a plant native to Southeastern Europe (Balkan Peninsula, Crimea), Western and Central Asia (Caucasus, Iran, Iraq). PC is a thorny shrub tree

with sphere-shaped, yellow/red/purple-colored fruits. Its young leaves are deep purple. When ripe, the leaves turn a dark green color (23-26).

It was presented research on green synthesis, characterization and antimicrobial properties of AuNPs from PC leaf in this article.

Materials and Methods

Materials

Green leaves of PC were collected from Mardin province in southeast Turkey. Tetrachloroauric acid ($\text{HAuCl}_4 \cdot 3\text{H}_2\text{O}$) was purchased from Alfa Aesar. Vancomycin, fluconazole and colistin antibiotics were purchased from Sigma Aldrich. *Escherichia coli* ATCC 25922, *Pseudomonas aeruginosa* ATCC27853, *Staphylococcus aureus* ATCC 29213, *Bacillus subtilis* ATCC 11774 and *Candida albicans* were also used in the study for the antimicrobial activities of AuNPs.

Preparation of Plant Extract

The green leaves of the PC plant were thoroughly washed with distilled water and dried under room conditions. 25 g of dry leaves were boiled in 500 ml of distilled water for 15 minutes. The extract was cooled to room temperature. Then, it was filtered with Whatman No. 1 filter paper and stored at +4 °C.

Synthesis of AuNPs

For the synthesis of AuNPs, 1 mM gold aqueous solution was prepared from the solid form of $\text{HAuCl}_4 \cdot 3\text{H}_2\text{O}$. 30 ml of PC leaf extract and 300 ml of $\text{HAuCl}_4 \cdot 3\text{H}_2\text{O}$ were mixed in a beaker and allowed to react stably at room temperature. The color change was observed within 30 minutes and the resulting dark solution was centrifuged at 10000 rpm for 10 minutes. The solid that remained at the bottom after centrifugation was washed several times with distilled water. The obtained AuNPs were left to dry in an oven at 80 °C for 48 hours. Then the dry part was ground into powder using a mortar and pestle.

Characterization of AuNPs

Agilent CARY 60 UV-visible spectrophotometer was used to confirm the synthesis of AuNPs by scanning the reaction mixture at wavelengths between 250-800 nm. The morphology, size, crystal structure and surface distributions of AuNPs were analyzed by FE-SEM (Quanta FEG240), TEM (Quanta), XRD (Rad B-DMAX II), EDX (Quanta FEG 240) and Zetasizer (Malvern Ins.Ltd.). FT-IR (Agilent Cary 630) was used to determine the functional groups present in the plant extract and the functional groups responsible for the reduction at the end of the reaction.

Antimicrobial Activity of AuNPs

The minimum inhibitory concentrations (MICs) of the resulting particles on gram-negative (*Escherichia coli* ATCC 25922, *Pseudomonas aeruginosa* ATCC27853) and gram-positive bacteria (*Staphylococcus aureus* ATCC 29213, *Bacillus subtilis* ATCC 11774) and *Candida albicans* were determined by microdilution using a 96-well microtiter plate. Mueller Hinton Broth for bacteria and RPMI (Growth Medium Used in Cell Culture) for yeast were added to the wells. AuNPs solution was added to the microplates containing the medium and microorganisms. 100 μL was taken each time and transferred to the next well. Then, a certain amount of microorganism solutions prepared and adjusted according to 0.5 McFarland was added to the microplates. It was incubated at 37 °C for 24 hours. The lowest concentration without growth after incubation was determined as the MIC value (27, 28). Moreover, a 1 mM $\text{HAuCl}_4 \cdot 3\text{H}_2\text{O}$ solution with commercial antibiotics vancomycin, colistin and fluconazole was used to compare the antimicrobial effects of AuNPs on *S. aureus*, *B. subtilis*, *E. coli*, *P. aeruginosa* and *C. albicans*.

Results and Discussion

UV-vis. Spectroscopy is an important method to determine the formation and stability of metal nanoparticles in an aqueous solution (29). It is seen that the UV-vis spectra of AuNPs change from light yellow to dark purple (Figure 1). These color changes occur

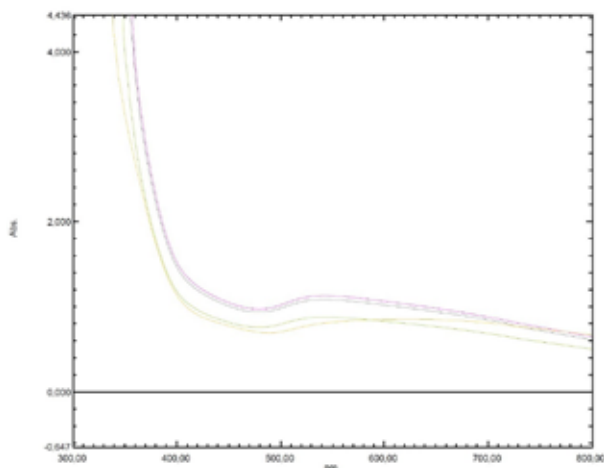
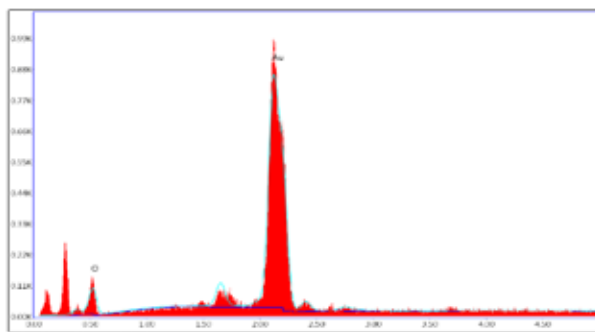


Figure 1. UV-Vis. absorbtion spectra of AuNPs

due to surface plasmon vibrations and AuNPs (30). As seen in the figure, AuNPs demonstrated a maximum peak around 535 nm. Daizy (31), Chandran et al. (32) and Kumar et al. (16) also reported peaks in the range of 537-548 nm for AuNPs.

According to the EDX data, the basic composition of the resulting AuNPs was confirmed to be gold (Figure 2). In addition, it was understood that AuNPs were in elemental structure. It can be said that the other peaks seen in Figure 2 were caused by the pollution from the PC leaf pulp. Similar results were obtained in green synthesis studies with extracts of *Pistia stratiotes* (33), *Cymbopogon citratus* (34), and *Artemisia absinthium* (35). From the EDX profile, weak signals such



Element	Wt %	Atomic %	Error %	Net Int.	Net Error %	K Ratio	Z	R	A	F
O K	28.51	80.99	18.51	81.14	5.44	0.0700	1.3213	0.7636	0.1887	0.0000
Au L	71.49	19.80	10.52	147.70	9.48	0.0867	0.8486	9.1279	8.2832	0.1318

Figure 2. The elemental composition of AuNPs by the EDX analysis

as oxygen and carbon may be due to biomolecules present on the surface of nanoparticles (36).

Surface morphology and particle size distribution of AuNPs obtained by green synthesis were revealed by FE-SEM and TEM measurements (Figures 3a, 3b, 4a and 4b). The FE-SEM and TEM results confirmed that the biosynthesized gold particles had nano dimensions. It was seen that the synthesized AuNPs were in clusters but not in direct contact with each other. This shows the stabilization of AuNPs. TEM images proved that the gold particles were predominantly spherical in shape (Figures 4a and 4b). Similar shaped AuNPs had also been reported in studies

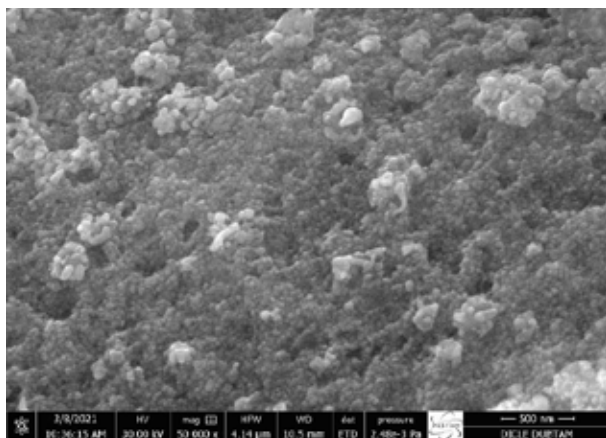


Figure 3a. FE-SEM image of AuNPs

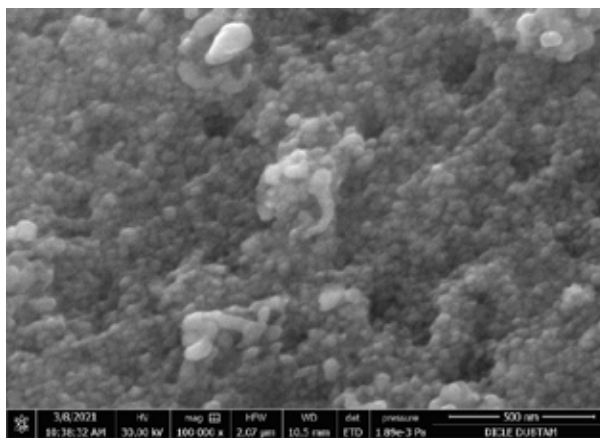


Figure 3b. FE-SEM image of AuNPs

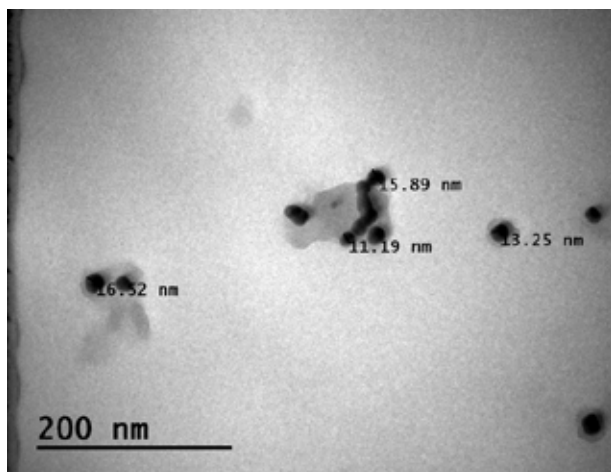


Figure 4a. TEM image of AuNPs

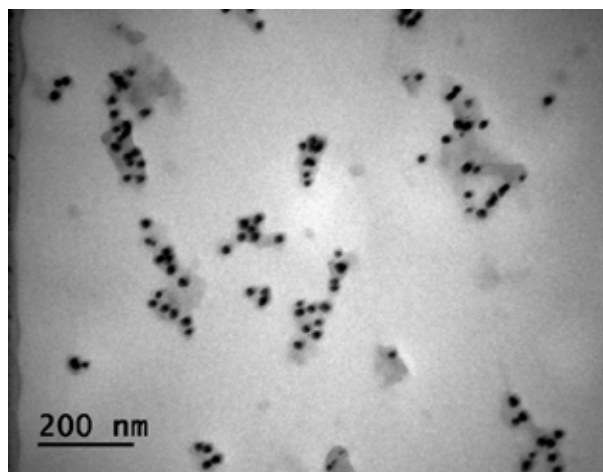


Figure 4b. TEM image of AuNPs

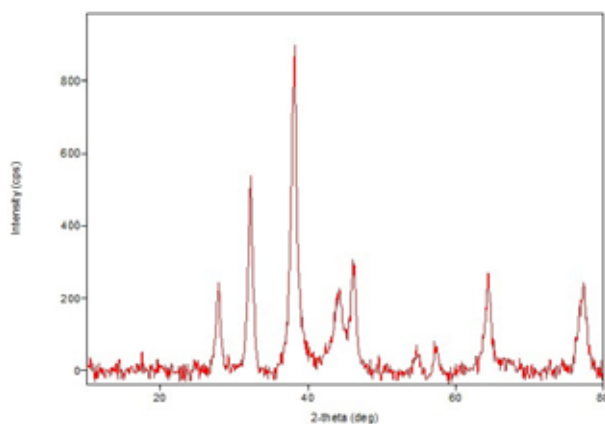


Figure 5. X-ray diffraction patterns of PC-AuNPs

of other researchers (18, 37, 38). The sizes of AuNPs were between 11.19-16.32 nm, with an average of 14.16 nm (Figure 4a).

The XRD spectrum for the synthesized AuNPs is shown in Figure 5. The peaks of $38.17^\circ(111)$, $44.06^\circ(200)$, $64.31^\circ(220)$ and $77.24^\circ(311)$ corresponding to 2θ in the XRD spectrum pattern show that

metallic gold has face-centered cubic crystal geometry (16, 39). The size of the nanoparticles was calculated as approximately 17.94 by the Debye-Scherrer equation.

When the biomolecules involved in the reduction during the formation of AuNPs are examined (Figures 6a and 6b), the absorption peak at 1636 cm^{-1} can be defined as amide I, which arises due to carbonyl ($\text{C}=\text{O}$) stretching vibrations in the amide ($-\text{C}(=\text{O})\text{N}=\text{}$) linkages of the proteins (37). It can be said that the absorption peak at 3326 cm^{-1} belongs to O-H and N-H stretching. Presumably, these functional groups are responsible for the reduction of metal ions. In some studies supporting the data of this research, NH and/or OH, $(\text{C}=\text{O})\text{NH}_2$ groups were reported to be responsible for the reduction (35, 40).

The average size of AuNPs with Zetasizer was determined as 103.8 nm (Figure 7a). The zeta potential (surface charge) of the biosynthesized AuNPs was found to be -27 mV (Figure 7b). Researchers who conducted similar studies with different plants reported that the zeta potential values of AuNPs were

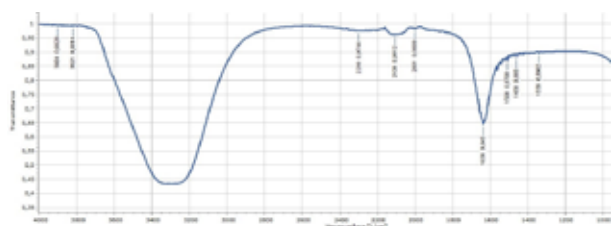


Figure 6a. FT-IR spectra of PC leaf extract

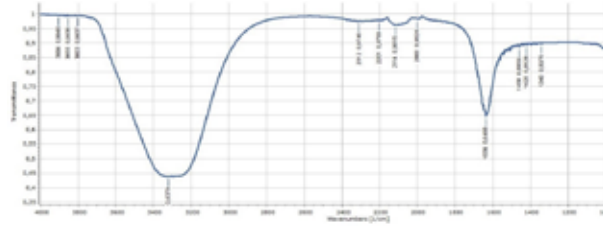


Figure 6b. FT-IR spectra of synthesized PC-AuNPs

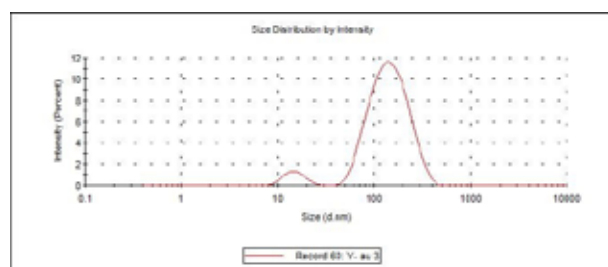


Figure 7a. Zeta size of AuNPs

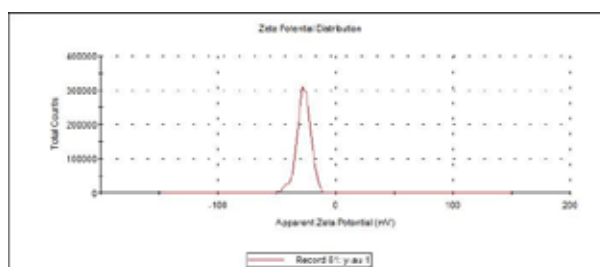


Figure 7b. Zeta potential of AuNPs

Table 1. MIC values of synthesized PC-AuNPs, $\text{HAuCl}_4 \cdot 3\text{H}_2\text{O}$ and antibiotics (mg / mL)

Microorganisms	PC-AuNPs	$\text{HAuCl}_4 \cdot 3\text{H}_2\text{O}$	Antibiotics
<i>Staphylococcus aureus</i> ATCC 29213	0.25	0.5	1
<i>Bacillus subtilis</i> ATCC 11774	0.125	0.25	1
<i>Escherichia coli</i> ATCC25922	1.0	1.0	2
<i>Pseudomonas aeruginosa</i> ATCC27853	0.5	1.0	1
<i>Candida albicans</i>	0.5	0.5	2

between -12 mV and -37 mV (41-45). The high negative value of the zeta potential is indicative of the high electrical charge on the surface of the particles in question due to the strong repulsion between the AuNPs. The high negative electric charge prevents aggregation and demonstrates the stability of the AuNP colloid (46).

Escherichia coli, *Staphylococcus aureus*, *Bacillus subtilis*, *Pseudomonas aeruginosa*, and *Candida albicans* are pathogenic microorganisms frequently encountered in foodborne diseases (47-51). In the study, it was observed that biosynthesized AuNPs significantly inhibited the growth of these microorganisms (Table 1). It was determined that AuNPs suppressed *Bacillus subtilis* more than the others. The antimicrobial mechanism of AuNPs is explained as cell wall, membrane, ribosome and mitochondrial damage and causing cell death by forming a thiol group in bacterial cells (52). Vijayakumar et al. (45) reported that different AuNP concentrations (12.5 mg/mL-100 mg/mL) significantly inhibited the proliferation of *Escherichia coli*, *Staphylococcus aureus*, *Bacillus subtilis*, and *Pseudomonas aeruginosa*. Bhau et al. (53), on the other hand, reported that AuNPs were more resistant (effective) against fungal species than bacteria.

Conclusion

With this research, aqueous green synthesis of AuNPs from PC leaf extract was reported for the first time. Therefore, economical, simple, fast and environmentally friendly AuNPs were synthesized using PC leaf extract. In addition, no toxic substance was used during this synthesis. EDX, XRD and UV-vis absorption confirmed the synthesis of AuNPs. FE-SEM and TEM studies revealed that AuNPs were generally spherical in shape and had an average size of about 14.16 nm. From the FT-IR spectra, the biomolecules responsible for the reduction and stabilization of AuNPs were found to be proteins present in the extract. In this study, it was determined that AuNPs had strong antimicrobial effects against foodborne pathogens even at low concentrations. However, new studies are recommended to reveal the effects of biosynthesized AuNPs on other microorganisms.

References

1. Khan N, Kumar D, Kumar P. Silver nanoparticles embedded guar gum/ gelatin nanocomposite: Green synthesis,

- characterization and antibacterial activity. *Colloid Interface Sci Commun* 2020; 35: 100242.
2. Tahir K, Nazir S, Ahmad A et al. Facile and green synthesis of phytochemicals capped platinum nanoparticles and in vitro their superior antibacterial activity. *J Photoch Photobio B* 2017; 166: 246-251.
 3. Khan Z, Al-Thabaiti SA. Green synthesis of zero-valent Fe-nanoparticles: Catalytic degradation of rhodamine B, interactions with bovine serum albumin and their enhanced antimicrobial activities. *J Photoch Photobio B* 2018; 180: 259-267.
 4. Pillai AM, Sivasankarapillai VS, Rahdar A et al. Green synthesis and characterization of zinc oxide nanoparticles with antibacterial and antifungal activity. *J Mol Struct* 2020; 128107.
 5. Baran MF, Saydut A. Gold nanomaterial synthesis and characterization. *Dicle University Journal of Engineering* 2019; 10(3): 1033-1040.
 6. Benedec D, Oniga I, Cuibu F et al. *Origanum vulgare* mediated green synthesis of biocompatible gold nanoparticles simultaneously possessing plasmonic, antioxidant and antimicrobial properties. *Int J Nanotechnol Nanomed* 2018; 13: 1041-1058.
 7. Chen H, Zhou K, Zhao G. Gold nanoparticles: From synthesis, properties to their potential application as colorimetric sensors in food safety screening. *Trends Food Sci Technol* 2018; 78: 83-94.
 8. Chellamuthu C, Balakrishnan R, Patel P, Shanmuganathan R, Pugazhendhi A, Ponnuchamy K. Gold nanoparticles using red seaweed *Gracilaria verrucosa*: Green synthesis, characterization and biocompatibility studies. *Process Biochem* 2019; 80:58-63.
 9. Badeggi UM, Ismail E, Adeloye AO et al. Green Synthesis of Gold Nanoparticles Capped with Procyanidins from *Leucosidea sericea* as Potential Antidiabetic and Antioxidant Agents. *Biomolecules* 2020; 10(3): 452.
 10. Elahi N, Kamali M, Baghersad MH. Recent biomedical applications of gold nanoparticles: A review. *Talanta* 2018; 184: 537-556.
 11. Kong F-Y, Zhang J-W, Li R-F, Wang Z-X, Wang W-J, Wang W. Unique Roles of Gold Nanoparticles in Drug Delivery, Targeting and Imaging Applications. *Molecules* 2017; 22(9):1445.
 12. Paidari S, Ibrahim SA. Potential application of gold nanoparticles in food packaging: a mini review. *Gold Bull* 2021; 54: 31-36.
 13. Jiménez-Pérez ZE, Singh P, Kim Y-J et al. Applications of Panax ginseng leaves-mediated gold nanoparticles in cosmetics relation to antioxidant, moisture retention, and whitening effect on B16BL6 cells. *J Ginseng Res* 2018; 42(3): 327-333.
 14. Krishnaswamy K, Vali H, Orsat V. Value-adding to grape waste: Green synthesis of gold nanoparticles. *J Food Eng* 2014; 142: 210-220.
 15. Awad MA, Eisa NE, Virk P et al. Green Synthesis of Gold Nanoparticles: Preparation, Characterization, Cytotoxicity, and Anti-bacterial Activities. *Mater Lett* 2019; 126608.
 16. Kumar PV, Kala SMJ, Prakash KS. Green synthesis of gold nanoparticles using *Croton Caudatus Geisel* leaf extract and their biological studies. *Mater Lett* 2019; 236(1): 19-22.
 17. Ramakrishna M, Rajesh Babu D, Gengan RM, Chandra S, Nageswara Rao G. Green synthesis of gold nanoparticles using marine algae and evaluation of their catalytic activity. *J Nanostructure Chem* 2015; 6(1): 1-13.
 18. Hamelian H, Hemmati S, Varmira K, Veisi H. Green synthesis, antibacterial, antioxidant and cytotoxic effect of gold nanoparticles using *Pistacia Atlantica* extract. *J Taiwan Inst Chem Eng* 2018; 93: 21-30.
 19. González-Ballesteros N, Prado-López S, Rodríguez-González JB, Lastra M, Rodríguez-Argüelles MC. Green synthesis of gold nanoparticles using brown algae *Cystoseira baccata*: Its activity in colon cancer cells. *Colloids Surf B Biointerfaces* 2017; 153: 190-198.
 20. Molnár Z, Bóday V, Szakacs G et al. Green synthesis of gold nanoparticles by thermophilic filamentous fungi. *Scientific Reports* 2018; 8: 3943.
 21. Javaid A, Oloketuyi SF, Khan MM, Khan F. Diversity of Bacterial Synthesis of Silver Nanoparticles. *BioNanoScience* 2017; 8(1): 43-59.
 22. Mohamed AA, Saad E, Fouda A, Elgamal MS, Salem SS. Extracellular biosynthesis of silver nanoparticles using *Aspergillus* sp. and evaluation of their antibacterial and cytotoxicity. *Journal of Applied Life Sciences International* 2017; 11(2):1-12.
 23. Horvath A, Christmann H, Laigret F. Genetic diversity and relationships among *Prunus cerasifera* (cherry plum) clones. *Botany* 2008; 86(11): 1311-1318.
 24. Kalyoncu İH, Ersoy N, Karali ME. Application Effects of Humidity and Different Hormone Doses on the Rooting of *Prunus cerasifera Pissardii Nigra* Softwood Top Cuttings. *Selcuk J Agr Food Sci* 2016; 30(2): 74-78.
 25. Popescu I, Caudullo G. *Prunus cerasifera* in Europe: distribution, habitat, usage and threats. In: San-Miguel-Ayanz, J., de Rigo, D., Caudullo, G., Houston Durrant, T., Mauri, A. (Eds.), *European Atlas of Forest Tree Species*. Publ. Off. EU, Luxembourg. 2016.
 26. Huo Y, Yan M, Zhao X, Zhu Z, Yuan Z. The complete chloroplast genome sequence of *Prunus Cerasifera* Ehrh. "Pissardii" (Rosaceae). *Mitochondrial DNA B Resour* 2019; 4(2): 3744-3745.
 27. Elshikh M, Ahmed S, Funston S et al. Resazurin-based 96-well plate microdilution method for the determination of minimum inhibitory concentration of biosurfactants. *Biotechnol Lett* 2016; 38(6): 1015-1019.
 28. Baran, A., Keskin, C. Green Synthesis of Nanoparticles and Anti-Microbial Applications: Academic Studies in Science and Mathematics – II, Ankara: Gece Academy, 2020; 1-18.
 29. Patra JK, Kwon Y, Baek K-H. Green biosynthesis of gold nanoparticles by onion peel extract: Synthesis, characterization and biological activities. *Adv Powder Technol* 2016; 27(5): 2204-2213.
 30. Mulvaney P. Surface Plasmon Spectroscopy of Nanosized Metal Particles. *Langmuir* 1996; 12(3): 788-800.

31. Daizy P. Green synthesis of gold and silver nanoparticles using *Hibiscus rosa sinensis*. *Physica E* 2010; 42: 1417-1424.
32. Chandran K, Song S, Yun S-I. Effect of size and shape controlled biogenic synthesis of gold nanoparticles and their mode of interactions against food borne bacterial pathogens. *Arabian Journal of Chemistry* 2019; 12: 1994-2006.
33. Anuradha J, Abbasi T, Abbasi SA. An eco-friendly method of synthesizing gold nanoparticles using an otherwise worthless weed pistia (*Pistia stratiotes* L.). *J Adv Res* 2015; 6(5): 711-720.
34. Murugan K, Benelli G, Panneerselvam C et al. *Cymbopogon citratus*-synthesized gold nanoparticles boost the predation efficiency of copepod *Mesocyclops aspericornis* against malaria and dengue mosquitoes. *Exp Parasitol* 2015; 153: 129-138.
35. Keskin C, Atalar NM, Baran MF, Baran A. Environmentally Friendly Rapid Synthesis of Gold Nanoparticles from *Artemisia absinthium* Plant Extract and Application of Antimicrobial Activities. *Iğdır University Journal of the Institute of Science and Technology* 2021; 11(1): 365-375.
36. Nishanthi R, Malathi S, John Paul S, Palani P. Green synthesis and characterization of bioinspired silver, gold and platinum nanoparticles and evaluation of their synergistic antibacterial activity after combining with different classes of antibiotics. *Mater Sci Eng C Mater Biol Appl* 2019; 96: 693-707.
37. Aromal SA, Vidhu VK, Philip D. Green synthesis of well-dispersed gold nanoparticles using *Macrotyloma uniflorum*. *Spectrochim Acta A Mol Biomol Spectrosc* 2012; 85(1): 99-104.
38. Maddinedi S, Mandal BK, Ranjan S, Dasgupt N. Diastase assisted green synthesis of size-controllable gold nanoparticles. *RSC Adv* 2015; 5(34): 26727-26733.
39. Suman TY, Radhika Rajasree SR, Ramkumar R, Rajthilak C, Perumal P. The Green synthesis of gold nanoparticles using an aqueous root extract of *Morinda citrifolia* L. *Spectrochim Acta A Mol Biomol Spectrosc* 2014; 118: 11-16.
40. Paul B, Bhuyan B, Dhar Purkayastha D, Dey M, Dhar SS. Green synthesis of gold nanoparticles using *Pogostemon benghalensis* (B) O. Kt. leaf extract and studies of their photocatalytic activity in degradation of methylene blue. *Mater Lett* 2015; 148: 37-40.
41. Shabestarian H, Homayouni-Tabrizi M, Soltani M, Namvar F, Azizi S, Mohamad R, Shabestarian H. Green Synthesis of Gold Nanoparticles Using *Sumac* Aqueous Extract and Their Antioxidant Activity. *Mat. Res.* 2017; 20(1): 264-270.
42. Raj S, Mali SC, Trivedi R. Green synthesis and characterization of silver nanoparticles using *Enicostemma axillare* (Lam.) leaf extract. *Biochem Biophys Res Commun* 2018; 503(4): 2814-2819.
43. Chellapandian C, Ramkumar B, Puja P, Shanmuganathan R, Pugazhendhi A, Kumar P. Gold nanoparticles using red seaweed *Gracilaria verrucosa*: Green synthesis, characterization and biocompatibility studies. *Process Biochem* 2019; 80: 58-63.
44. Mohammad I. Gold nanoparticle: An efficient carrier for MCP I of *Carica papaya* seeds extract as an innovative male contraceptive in albino rats. *J Drug Deliv Sci Technol* 2019; 52: 942-956.
45. Vijayakumar S, Vinayagam R, Anand MAV et al. Green synthesis of gold nanoparticle using *Eclipta alba* and its antidiabetic activities through regulation of Bcl-2 expression in pancreatic cell line. *J Drug Deliv Sci Technol* 2020; 58: 101786.
46. Mapala K, Pattabi M. *Mimosa pudica* Flower Extract Mediated Green Synthesis of Gold Nanoparticles. *NanoWorld J* 2017; 3(2): 44-50.
47. Olsvik Ø, Wasteson Y, Lund A, Hornes E. Pathogenic *Escherichia coli* found in food. *Int J Food Microbiol* 1991; 12(1): 103-113.
48. Middleton SJ, Coley A, Hunter JO. The role of faecal *Candida albicans* in the pathogenesis of food-intolerant irritable bowel syndrome. *Postgrad Med J* 1992; 68(800): 453-454.
49. Le Loir Y, Baron F, Gautier M. *Staphylococcus aureus* and food poisoning. *Genet Mol Res* 2003; 2 (1): 63-76.
50. Hitosugi M, Hamada K, Misaka K. Effects of *Bacillus subtilis* var. natto products on symptoms caused by blood flow disturbance in female patients with lifestyle diseases. *Int J Gen Med* 2015; 8: 41-46.
51. Mostafa AA, Al-Askar AA, Almaary KS, Dawoud TM, Sholkamy EN, Bakri MM. Antimicrobial activity of some plant extracts against bacterial strains causing food poisoning diseases. *Saudi J Biol Sci* 2018; 25(2): 361-366.
52. Sunderam V, Thiyagarajan D, Lawrence AV, Mohammed SSS, Selvaraj A. In-vitro antimicrobial and anticancer properties of green synthesized gold nanoparticles using *Anacardium occidentale* leaves extract. *Saudi J Biol Sci* 2019; 26(3): 455-459.
53. Bhau BS, Ghosh S, Puri S, Borah D, Sarmah DK, Khan R. Green synthesis of gold nanoparticles from the leaf extract of *Nepenthes khasiana* and antimicrobial assay. *Adv Mater Lett* 2015; 6(1): 55-58.

Correspondence

Abdulkerim Hatipoğlu
Department of Nutrition and Dietetics,
Faculty of Health Sciences,
Mardin Artuklu University,
Mardin, Turkey, 47000
Email: abdulkerimhatipoglu@artuklu.edu.tr